



# **Practical Evaluation of a Full-Bridge Phase-Shift-Modulated ZVS DC-DC Converter**

Nithin George<sup>1</sup>, Elizabeth Sebastian<sup>2</sup>, Reenu George<sup>3</sup>

P.G.Scholar, Department of Electrical and Electronics Engineering, Mar Athanasius College of Engineering,  
Kothamangalam, Kerala, India<sup>1</sup>

Professor, Department of Electrical and Electronics Engineering, Mar Athanasius College of Engineering,  
Kothamangalam, Kerala, India<sup>2</sup>

Assistant Professor, Department of Electrical and Electronics Engineering, Mar Athanasius College of Engineering,  
Kothamangalam, Kerala, India<sup>3</sup>

**ABSTRACT:** The practical performance evaluation of a full-bridge phase-shift-modulated DC-DC converter is presented in this paper. The converter has the property of zero voltage switching (ZVS) using the transformer leakage inductance, without the need for any additional components. The implementation aspects of the converter are discussed, including the design of the high frequency transformer and LC filter, and configuration of the signal generation system and the driving circuits. The experimental results from a 450 W prototype are provided and these support the case for ZVS taking place in the converter. The effectiveness of the design is validated by the full load efficiency of 92% that was given by the prototype.

**KEYWORDS:** Full-bridge DC-DC converter, zero voltage switching, phase-shift-modulation, practical evaluation.

## **I. INTRODUCTION**

A DC-DC converter forms the main part of a Switch Mode Power Supply (SMPS), fuel cell power conditioning unit, battery charger, etc. Such a DC-DC converter may be of isolated or non isolated type. Isolated DC-DC converters can employ topologies including forward, flyback, push-pull, half-bridge and full-bridge [1]. Of the different topologies available, the full-bridge converter is quite popular due to its symmetric mode of operation and large power handling capability.

For full-bridge DC-DC converter different switching techniques are available; of these, the Phase Shift Modulation (PSM) technique is widely used. The main reason for this is the soft switching i.e., Zero Voltage Switching (ZVS) that is offered by the PSM technique. No extra components are needed and the circuit parasitics: the device capacitance and transformer leakage inductance are used for attaining ZVS. PSM technique and the design considerations were first detailed in [2].

This paper discusses various aspects associated with design and implementation of a PSM full-bridge DC-DC converter having a full load capacity of about 450W. The converter uses a high step ratio of 1: 6 and such ratios are widely seen in fuel cell power conditioning systems [3]. The design aspects of the transformer and the LC filter at the output are discussed in detail. Also the implementation aspects like generation of signals, isolation between the HV and LV circuits, and driving requirements are given a brief look-through. Through the experimental results, the evidence for ZVS is presented

## II. THE CONVERTER

The full-bridge DC-DC converter is sketched in Fig. 1(a). In PSM technique, the two legs of the active bridge are operated with a phase shift  $p^\circ$  as shown in Fig. 1(b). The phase shift angle and duty cycle of the converter are related by:

$$D = \frac{p^\circ}{180^\circ} \quad (1)$$

The phase shift operation results in the discharge of the switch output capacitance and forcing of the anti parallel diode of the switch into conduction even before the switch itself starts to conduct. Thus the switch is turned on at zero voltage.

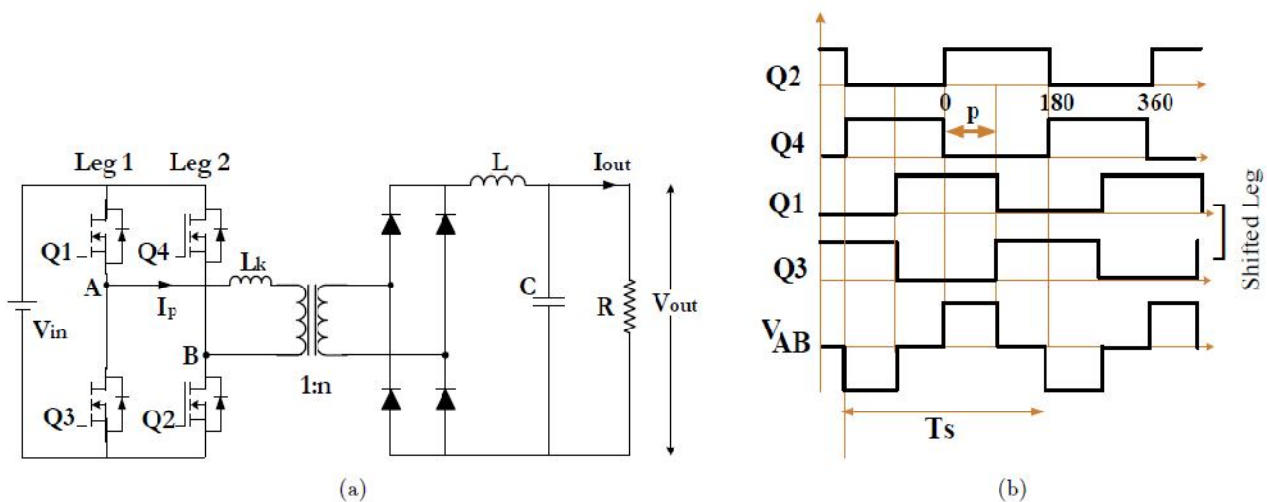


Fig. 1: (a) Circuit configuration of a full-bridge DC-DC converter. (b) Phase-Shift-Modulation switching of the converter.

The energy stored in leakage inductance  $L_k$  is used to discharge the device output capacitances and force conduction of the body diodes of Q2 and Q4. If the load current is small, the energy stored may not be enough for this process and ZVS may not take place. The critical value of load current below which ZVS is lost is found to be inversely proportional to the magnitude of  $L_k$  [2]. In the case of devices Q3 and Q1, the energy stored in the filter inductance  $L$  is also available, in addition to that stored in  $L_k$ , to discharge the output capacitances and force conduction of the diodes. Thus even for light loads ZVS can be achieved for these two devices.

In PSM switching of the converter, the duty cycle of the voltage at the secondary is found to be smaller than that of the primary. This is due to the finite slope associated with the rise and fall of transformer primary current  $I_p$ . The effective duty cycle  $D_e$  (or duty cycle at secondary) is given as [4]:

$$D_e = \frac{D}{\frac{R_d}{R} + 1} \quad (2)$$

where  $R_d = 4 n^2 L_k f_s$ ,  $f_s$  indicates the switching frequency, and  $R$  the load resistance. From (2) it can be inferred that a higher value of  $L_k$  results in a lower  $D_e$ . Thus the choice for  $L_k$  is influenced by conflicting factors: ZVS and gain reduction.

Finally, the relationship between  $V_{in}$  and  $V_{out}$  will have to be defined:



# International Journal of Advanced Research in Electrical, Electronics and Instrumentation Engineering

(An ISO 3297: 2007 Certified Organization)

Vol. 3, Special Issue 5, December 2014

$$V_{out} = V_{in} \cdot N \cdot D_e \quad (3)$$

which is similar to that of a buck/forward converter.

### III. IMPLEMENTATION AND DESIGN ASPECTS

It is intended to develop a DC-DC full bridge converter with the specifications as given in Table 1(a). Based on the above requirements the preliminary component choices are made and they are listed in Table 1( b).

#### A. Transformer

Once a core material is chosen, the turns ratio 1: n and the number of turns in the primary and secondary windings will have to be determined. The value of n can be found out using the relationship:

Parameter	Value
Input voltage $V_{in}$	60 V (nominal)
Output voltage $V_{out}$	300 V (nominal)
Full load power output	450 W
Switching frequency $f_s$	20 kHz
Automatic regulation	none

(a)

Component	Choice - Description
Switching device	IRFP 264N - MOSFET 250V, 40A
Transformer core	EPCOS Pot Core N87 - $B_m = 490 \text{ mT}$ , up to 500 kHz
Fast recovery diode bridge	MUR 4100E - 1000V, 4A , $t_{rr} = 75 \text{ ns}$

(b)

Table 1: (a) Converter Parameters. (b) Preliminary component choices.

$$n \approx \frac{V_{out \max}}{V_{in \min} \cdot D_{\max}} (1 + R_d/R) \quad (4)$$

Since  $V_{out}$  is to be 300 V,  $n = 6$  is chosen. This will ensure the nominal output voltage even at a reduced  $V_{in}$  of about 55 V.

The rms value of induced emf in the transformer primary winding can be written as:

$$E_p = 4.44 f_s B_m A_i N_p \quad (5)$$

where  $B_m$  is the maximum flux density permissible in the core,  $A_i$  the iron area and  $N_p$  the number of turns in the primary. This equation is based on operation of the transformer with a sinusoidal supply. The transformer in the instant case is subjected to quasi square wave  $V_{AB}$  as shown in Fig. 1(b) and the rms value of fundamental component of this waveform is given by [5]:

$$V_f = \frac{4}{\pi\sqrt{2}} \cdot V_{in} \cdot \sin \left[ \frac{\pi}{2}(1 - D) \right] \quad (6)$$

The design of the transformer is based on the assumption that it is subjected to this fundamental component of voltage  $V_f$ . For  $V_{in} = 60 \text{ V}$  and duty cycle  $D=1$ , the value would be obtained as  $E_p = V_f = 54 \text{ V}$  from (6). Now a core size 62/49, which has an iron area  $A_i$  of 570 sq. Mm, is chosen [6]. This is a preliminary choice, later on if this core is found not to have suitable window area to accommodate the windings, the next higher core size may be chosen.



## International Journal of Advanced Research in Electrical, Electronics and Instrumentation Engineering

(An ISO 3297: 2007 Certified Organization)

Vol. 3, Special Issue 5, December 2014

Further, the B-H curve of the transformer core material has to be looked into, and avoiding the saturation region, a maximum flux density  $B_m$  of 100 mT is chosen for operation. Substituting for all the known values in (5),  $N_p$  may be chosen as 13. Also the number of turns in the secondary,  $N_s$  may be determined as 78 without any doubt.

With regard to the gauge chosen for the windings, the primary and secondary currents at full loads may be determined, and gauge of wires chosen from a gauge table [7]. A check is performed to ensure that the windings would be accommodated in the window area of the pot core and for this the following relation may be used:

$$A_w = \frac{a_p N_p + a_s N_s}{K_w} \quad (7)$$

where  $a_p$ ,  $a_s$  is the cross sectional area of the 1<sup>o</sup> and 2<sup>o</sup> winding wires respectively and  $K_w$  is the window factor, a value lying between 0.6 and 0.4.  $a_p$  and  $a_s$  may be obtained from the gauge tables itself and a substitution in the above relationship gives the window area  $A_w$ . If the window area calculated is more than the actual window area, the next higher core size will have to be chosen and design repeated. If the calculated window area is less, either this design may be adopted or a redesign may be made with a smaller core size.

Once the transformer is wound, immediately the leakage inductance is determined by conducting short circuit test using an LCR meter. The parameters of the transformer are summarized in Table. 2( a).

Parameter	Value	Brief Description
1 <sup>o</sup> gauge (SWG)	14	$a_p = 3.24 \text{ mm}^2$
2 <sup>o</sup> gauge (SWG)	20	$a_s = 0.657 \text{ mm}^2$
$L_k$	$2 \mu H$	—

(a)

Parameter	Choice	Consequence
$L$	1.6 mH, air core	$I_{LB \text{ max}} = 0.703 \text{ A}$
$C$	220 $\mu F$ , electrolytic	$\Delta V_o = 20 \text{ mV}$

(b)

Table 2: (a) Transformer parameters. (b) LC filter parameters.

### B. LC Filter

Once the transformer is designed, the next significant design is associated with the 2<sup>nd</sup> order LC filter at the output. The value of inductance L determines the boundary of discontinuous conduction mode. If the value of inductance is large, the current value which forms the boundary between continuous and discontinuous conduction mode will be smaller, i.e., continuous conduction mode can be assured for smaller values of load currents [5]. The relationship between the L and the maximum value of boundary load current is given by:

$$L = \frac{nV_{in}}{16f_s I_{LB \text{ max}}} \quad (8)$$

Usually converters are operated in continuous conduction mode and the expression (2) is only valid during this mode. Also the small signal model during the two modes is quite different.

Capacitor value is chosen based on the maximum output voltage ripple that can be tolerated. The expression for maximum peak to peak output voltage ripple is given by:

$$\Delta V_o = \frac{nV_{in}}{128f_s^2 LC} \quad (9)$$

Now based on the requirements, values are chosen for L and C, and the choices with their consequences are listed in Table. 2(b).

# International Journal of Advanced Research in Electrical, Electronics and Instrumentation Engineering

(An ISO 3297: 2007 Certified Organization)

Vol. 3, Special Issue 5, December 2014

### C. Gating Signal Generation

A 16 bit PIC microcontroller, dsPIC30F2010, is used to generate the four gating signals for the switches. This PIC has an inbuilt PWM module and using this in conjunction with an infinite loop algorithm, the PSM signals are generated.

In order to prevent any chance of unreliable operation of the microcontroller, the ground of the 5 V supply given to the PIC is kept isolated from the supply ground of the driver and DC rail. For transmission of signals from one circuit to another, an optocoupler is used. HCPL 2630 is the IC used for this purpose in the instant case, and it can handle two channels per IC.

### D. Driving

Considering a single leg of the full bridge DC-DC converter, while the lower device can be driven by any source as long as it can supply the required current, the upper device cannot be driven so due the floating nature of its source. Thus in order to drive it a driver IC is required. IR2110 is one such IC that can be used to drive both the devices in a single leg. For the upper device it employs a bootstrap mechanism and the gate voltage of the device would be 15-12 V higher than the DC rail voltage  $V_{in}$ . It may be noted that the ground of driver IC is made common with the DC rail. The connection of the IR2110 IC with the switching devices is illustrated in Fig. 2(a), while Fig. 2(b) shows the signal flow path from the microcontroller to the device gate.

## IV. EXPERIMENTAL RESULTS

Fig. 3(a) shows the driving signals given to the upper devices Q4 and Q1. The waveforms were taken with the DC rail OFF, limiting the amplitude of the driving voltages to 12 V. Math shows CH3-CH4 and are a scaled version of transformer primary voltage  $V_{AB}$ . The evidence for ZVS in a switch is obtained by observing its gate voltage together with the drain-to-source voltage  $V_{ds}$ . ZVS is obtained at turn ON and if  $V_{ds}$  goes low even before the gate-to-source voltage  $V_{gs}$  goes high, it

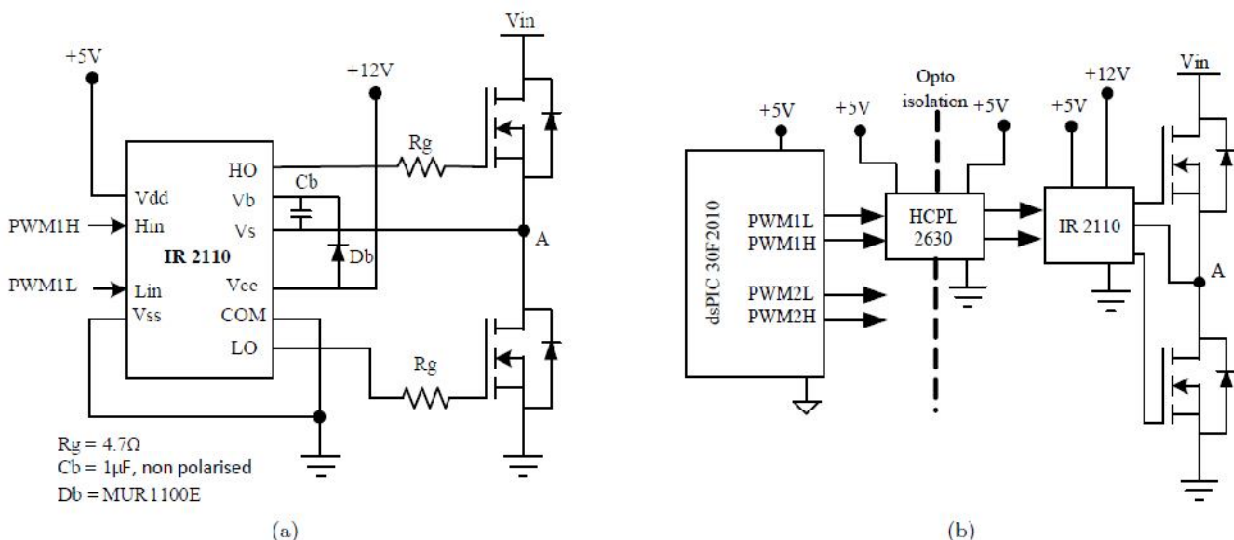


Fig. 2: (a) Interconnection of IR2110 with the switching devices. (b) Signal flow path from PIC to the switch gate.

indicates conduction of diodes and hence ZVS. The waveforms in relation to this for Q3 at full load condition are shown in Fig. 3(b) and ZVS can be observed clearly.

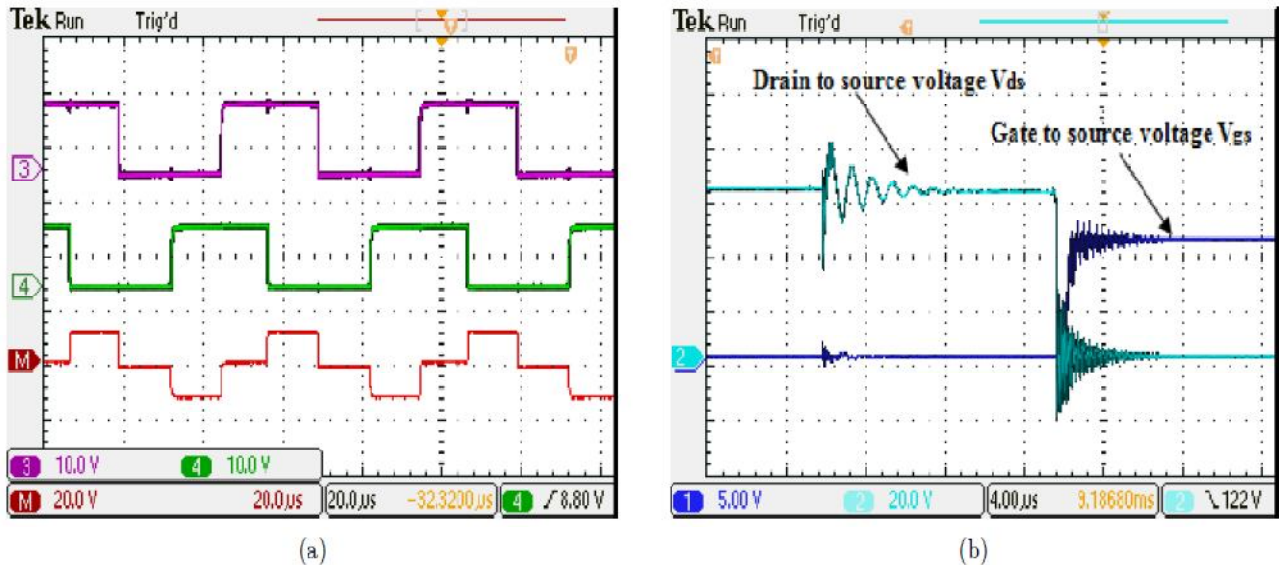


Fig. 3: (a) Gating voltage given to the upper devices Q1 and Q4 for duty cycle  $D=50\%$ , with DC rail being OFF (CH3 and CH4 respectively). (b) Zero voltage switching for switch Q3 at full load.  $CH1 = V_{ds}$  and  $CH2 = V_{gs}$ . (Trigger points overlap).

The primary voltage  $V_{AB}$  waveform, determined by subtracting  $V_B$  from  $V_A$ , is shown in Fig. 4. The primary current  $I_p$  waveform is also shown. The waveforms in Fig. 4(a) are for  $V_{out} = 299$  V and  $R = 200$  ohms i.e., full load. The waveforms may be compared to the theoretical prediction in [2] and the similarity noted. The conduction of diodes prior to conduction of devices is clear and yet another evidence of ZVS is obtained. Fig. 4(b) shows the same waveforms for a duty cycle of 50 % and  $I_{out}$  of 0.825 A, with  $R=200$  ohms. Lack of ZVS is clear from the waveforms.

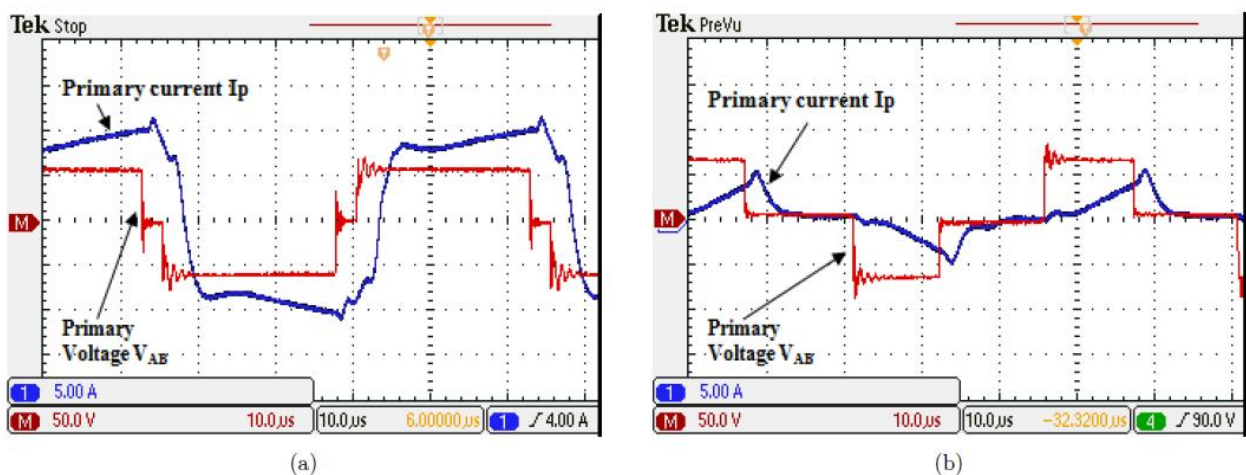


Fig. 4: (a) Primary voltage  $V_{AB}$  (Math) and primary current  $I_p$  (CH1) for full load. (Trigger points overlap). (b) Primary voltage  $V_{AB}$  (Math) and primary current  $I_p$  (CH1) for a  $I_{out}$  of 0.825 A. (Trigger points overlap).

The filtered output voltage together with the current drawn from the input DC supply is shown in Fig. 5(a). The waveform is taken at  $D=90\%$ ,  $V_{out} = 299$  V and  $R = 200$  ohms. The efficiency curve of the converter is shown in Fig.

# International Journal of Advanced Research in Electrical, Electronics and Instrumentation Engineering

(An ISO 3297: 2007 Certified Organization)

Vol. 3, Special Issue 5, December 2014

5(b). It can be seen that beyond 300 W the curve is almost a constant at 92 %, showing the ideal loading region for the present converter design.

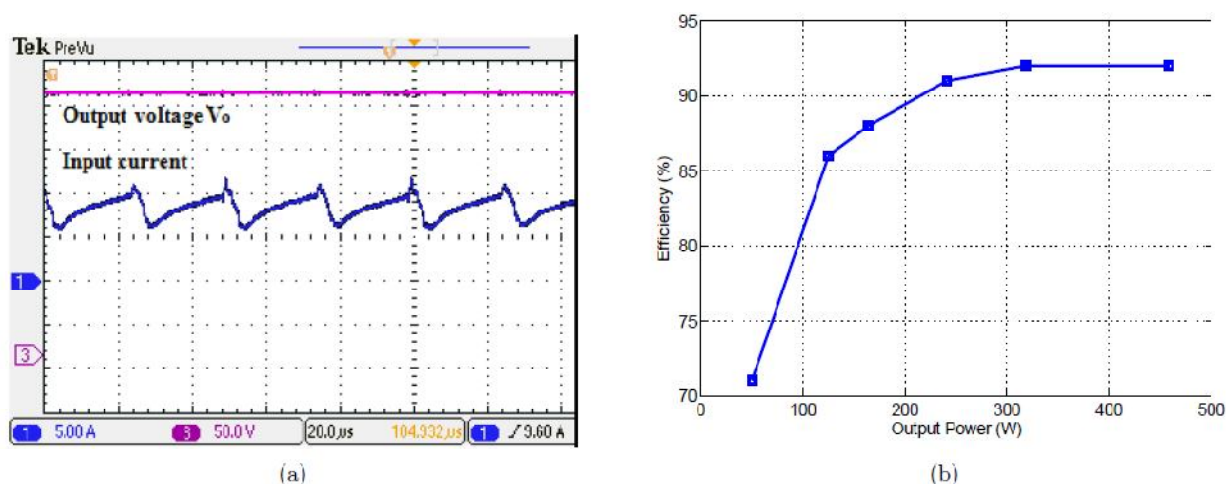


Fig. 5: (a) Filtered output voltage of the converter (CH3) and the input supply current (CH1).  $R = 800 \Omega$  and  $D=50\%$ .  
(b) The efficiency curve of the converter.

## V.CONCLUSION

This paper has demonstrated design, implementation and practical evaluation of a zero voltage switching, phase-shift-modulated, full-bridge DC-DC converter. The implementation aspects have been elaborated in detail with special emphasis being given to high frequency transformer design. The driver circuitry together with the signal generation mechanism has been given a detailed look-through. The signal flow path through the optocoupler and its need has also found a mention in the paper.

Since practical evaluation was the main objective, a significant amount of results in this regard has been presented. Two evidences for ZVS in the converter switches have been obtained from the experimental study. The efficiency curve of the converter shows a maximum efficiency of 92 % at full load, indirectly supporting the case for ZVS.

## REFERENCES

- [1] R. W. Erickson and D. Maksimovic, *Fundamentals of Power Electronics*, 2nd edition. New York, Kluwer Academic Publishers, 2004.
- [2] J.A. Sabate, V. Vlatkovic, R. B. Ridley, F. C. Lee and B. H. Cho, "Design considerations for high-voltage high-power full-bridge zero voltage switched PWM converter," in *Proceeding of 5th Annual Applied Power Electronics Conference and Exposition*, 1990, pp. 275-284.
- [3] J. Wang, F. Z. Peng, J. Anderson, A. Joseph and R. Buffenbarger, "Low Cost Fuel Cell Converter System for Residential Power Generation," *IEEE Transactions on Power Electronics*, vol. 19, no. 5, pp. 1315-1322, Sept. 2004.
- [4] V. Vlatkovic, J. Sabate, R. B. Ridley, F. C. Lee and B. H. Cho, "Small signal analysis of the phase-shifted PWM Converter," *IEEE Transactions on Power Electronics*, vol. 7, no. 1, pp. 128-135, Jan. 1992.
- [5] N. Mohan, T. M. Undeland, W. P. Robbins, *Power Electronics Converters, Application and Design*, 3rd edition, Wiley-India, New Delhi, 2003.
- [6] *EPCOS Data Book- Ferrites and Accessories*, TDK, U.S.A, 2013.
- [7] *Practical Electronics/SWG-Wikibooks* [Online]. Available: <http://en.wikibooks.org/wiki/Practica/Electronics/SWG>